

# Analysis of Myocardial Infarction Using Wavelet Transform and Multiscale Energy Analysis

Sushree Satvatee Swain  
Department of Electrical Engineering  
National Institute of Technology  
Rourkela, India  
ssatvatee16@gmail.com

Dipti Patra  
Department of Electrical Engineering  
National Institute of Technology  
Rourkela, India  
dpatranitrkl.ac.in

**Abstract—** Myocardial Infarction (MI) is otherwise termed as heart attack, occurs when blood supply stops to certain artery or to some portion of arteries. MI is depicted in elevated ST-segment, wide pathological Q wave and inversion of T wave in electrocardiogram (ECG). This paper presents a multiscale energy based method for detection of MI. Detection of MI by consideration of fewer ECG leads requires prior information of the pathological characteristics of the disease. Thus, here we have considered all the 12 leads of the ECG signal simultaneously for detection of MI. Wavelet transform of all the leads of MI decomposes the signal into subbands of different order. The multiscale energy of all the bands are computed and the normalized multiscale energy of the wavelet coefficients are considered. The pathological structure present in the ECG data alters the covariance structure of the subband matrix and thus changes in the feature parameters of the signal occur, which leads to detection of MI. The results are presented using the standard MI ECG data from PTB diagnostic database.

**Keywords:-** Myocardial Infarction; electrocardiogram; multiscale energy; subband matrix; covariance

## I. INTRODUCTION

The graphical representation of electrical activity of the cardiac muscles over a period of time is termed as ECG [1]. ECG signal plays an important role in diagnosis of the cardiac condition of the patient. From the captured ECG recordings, physicians trace the cardiac condition of the human being. By seeing the ECG records trained cardiologists trace the abnormality present in the functioning of the heart. It is quite strenuous task for the cardiologists to detect the cardiac disorder by seeing the very long ECG recordings manually. Thus automated earlier detection and classification techniques of cardiac abnormality are highly essential.

Myocardial infarction (MI) is commonly referred as heart block or heart attack, which is the main cause of death among all cardiovascular disorders [1] [2]. MI occurs due to occlusion of one of the coronary artery or some small branches of the artery. The pathogenesis of MI occurs due to progressive development of atherosclerotic plaques along the inside wall of the artery. This is followed by deprivation of oxygen and important nutrients to the myocardial cell leading to loss of perfusion to the myocardium. This leads to deposition of blood platelets, red blood cells and fibrin and

thus forming a local blood clot otherwise known as thrombus [3]. Sometimes thrombolytic substances are detached from the main artery and are driven to some distal arterial tree and are deposited there. This is followed by blocking of artery or some portion of the artery which is termed as formation of coronary embolus. This is followed by interruption of blood flow to the artery or some branches of the artery called as myocardial necrosis. Complete necrosis of the myocardium at risk takes about 4 to 5 hours to happen. Myocardial injury is detected when the level of sensitive and specific biomarkers such as creatine kinase (CKMB) and cardiac Troponin T increases in the blood [3]–[5].

ECG signal consists of P wave, QRS complex and the T wave. P wave results from depolarization of the atria. QRS complex is produced due to depolarization of the ventricles and T wave is the result of repolarization of the ventricles. Certain changes in normal ECG wave occur on the onset of the MI. These changes include ST segment elevation, appearance of pathological Q wave and inversion of T wave. Thus MI is categorized as ST segment elevated and non ST segment elevated MI (STEMI and non-STEMI). The important feature for earlier detection of MI is ST segment. There are mainly three stages in MI namely injury, ischemia and infarction [6]. Elevation of the ST segment occurs at the stage of myocardial ischemia. Thus ST segment analysis is the key feature for earlier detection of MI. In a standardized 12-lead ECG system each lead views the heart at a specific angle. In MI the multilead recordings of heart deviate from its normal healthy characteristics. The changes occur in different ECG leads. Thus it is required to investigate all the 12 leads at one time.

Previously various methods have been proposed for the detection of MI. Time domain methods are used for analysis of MI [7]–[9]. ST-segment analysis [10] [11] and the wavelet transform based methods [12] [13] have been adopted for detection of MI. Some researchers have developed neural network approach [14]–[16] for detection and localization of MI. Some of these techniques use modelling based schemes by means of training and testing the system. Generally these modelling based techniques use only few ECG leads for

analysis of MI. The analysis is done on some portion of ECG signal such as ST-segment, ST-T complex instead of the entire ECG segment. This needs the accurate and exact detection of ST-segment. This process requires prior information about the presence of MI in some of the selected leads. Various categories of MI are present in different ECG leads. Thus monitoring all the 12 leads at one time will produce better accuracy in detection and localization of MI. In this study wavelet transform and multiscale energy analysis [17] [18] is used for detection of MI. Here the work is carried out taking the MI ECG signals from PTB diagnostic database. Implementation on real data on human subjects needs approval of the medical board.

## II. METHODOLOGY

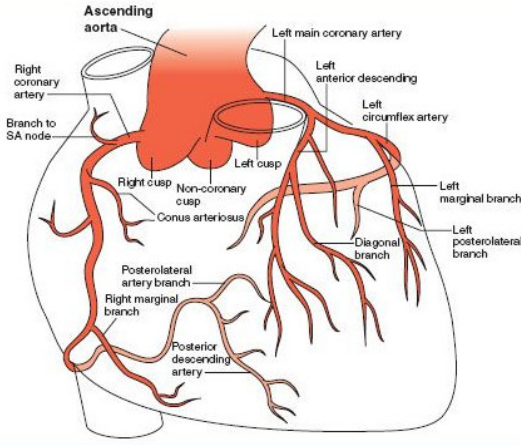


Fig. 1: Coronary arteries of human heart and 12-standard ECG leads in different planes

Coronary arteries distribution and their anatomic relations with ECG leads are shown in Fig. 1. The left main coronary artery branches into left anterior descending and left circumflex artery. These two arteries supply blood to the anterior left ventricle (LV), the lateral and posterior LV walls, the interventricular septum, and the apex. The right coronary artery (RCA) supplies blood and nutrients to right ventricle, inferior wall of LV, part of the posterior wall of the LV through the posterior descending artery and posterior interventricular septum [1]. Any of the above arteries may have occlusions and undergo under myocardial injury. MIs are categorised into anterior MI, inferior MI, posterior MI, and left lateral MI. Anterior MI is reflected in the ECG leads V1, V2, V3, and V4 and the inferior MI is diagnosed from ECG leads II, III, and aVF. The left lateral MI are reflected pathologically in ECG leads I, aVL, V5, and V6. Posterior MI is the result of necrosis in RCA. ECG leads are unable to trace the behaviour of the posterior wall. Thus, it is analysed by considering the reciprocal changes in the anterior lead V1.

In Fig. 2, block diagram of sequences of processes for detection of MI is presented. The detection block includes

preprocessing, wavelet transform, multiscale energy analysis, and classification. The preprocessing stage consists of filtering technique and then frame based segmentation has been performed. A moving average filter [19] has been used to discard the artifacts such as base line wanders, muscle artifacts, and the baseline drift. The frame-based segmentation of 12-lead ECG is done to capture the interlead, intrarhythm, and intersample correlation information. These are very vital information to diagnose different types of cardiac diseases [11].



Fig. 2: Detection of MI from multilead ECG Wavelet Transform

Fourier transform (FT) is performed to represent a signal as a summation of sinusoids and it is the signal representation in frequency domain. But the wavelet transform is the representation of signal in both time and frequency domains [12]. To detect the onset of MI in ECG recording both time and frequency domain analysis is needed. Thus wavelet Transform is adopted to trace the point at which the abrupt changes have been occurred in the frequency domain at a particular instant of time. The wavelets are compactly supported small waves confined between a finite period of time. A discrete wavelet transform (DWT) generally uses a dyadic grid  $a = 2^m$ ,  $m \in \mathbb{Z}$  and  $b = nb_02^m$ ,  $n \in \mathbb{Z}$ . Assuming  $b_0 = 1$

$$\Psi_{m,n}(t) = 2^{-m/2}\Psi(2^{-m}t - n) \quad (1)$$

The scaling function is defined as

$$x(t) = \sum_{n=-\infty}^{\infty} S_{M,n}\Phi_{M,n}(t) + \sum_{m=-\infty}^M \sum_{n=-\infty}^{\infty} W_{m,n}\Psi_{m,n}(t) \quad (2)$$

corresponding to the wavelet

$$\Phi_{m,n}(t) = 2^{-m/2}\Phi(2^{-m}t - n) \quad (3)$$

where

$S_{M,n} = \langle x(t)\Phi_{M,n}(t) \rangle$  : Approximation coefficients

$W_{m,n} = \langle x(t)\Psi_{m,n}(t) \rangle$  : Detail coefficients

$M$  : Decomposition level

Signal approximation at level  $M$  is expressed as

$$x_M(t) = \sum_{n=-\infty}^{\infty} S_{M,n}\Phi_{M,n}(t) \quad (4)$$

Detail coefficient of the signal at scale  $m$  is expressed as

$$d_m(t) = \sum_{n=-\infty}^{\infty} W_{m,n}\Psi_{m,n}(t) \quad (5)$$

and the signal is the summation of the signal approximation and the detail coefficient.

$$x(t) = x_M(t) + \sum_{m=-\infty}^M d_m(t) \quad (6)$$

After performing the wavelet transform several features of ECG signal will be confined to different decomposition level of the signal.

Wavelet analysis of an ECG signal with  $M$ -level decomposition using suitable mother wavelet produces  $n^{th}$  wavelet coefficient at the  $M^{th}$  level [12]. This wavelet analysis is based upon the multiresolution pyramidal decomposition technique and it decomposes the signal upto  $M + 1$  subbands. For  $k^{th}$  ECG lead the decomposition results with an approximation subband coefficients,  $cA_{M,n}^k$  at level  $M$  and with detail subbands,  $cD_{m,n}^k$  at level  $m$  where  $m = 1, 2, \dots, M$ . The approximation coefficient is obtained by taking the inner product of the input multilead ECG signal with the scaling function. The detail coefficient is obtained by taking the inner product of the input ECG signal with the wavelet function. In this work a six level wavelet decomposition of 12 lead ECG signal is adopted. The diagnostic and pathological information are distributed over different wavelet subbands basing upon their bandwidth and frequency distribution. The lower frequency subbands contain most significant information of the ECG signal whereas the higher frequency subbands contain least significant information.

### Multiscale Energy Analysis

Wavelet coefficients of all 12 ECG leads with  $M$ -level wavelet decomposition are represented in  $M + 1$  subband matrices. The columns of the subband matrix represent the corresponding leads of ECG and the rows represent the coefficients of the subband. Considering  $S_{M,n} = A_{M,n}$  and  $W_{m,n} = D_{m,n}$ , the approximation subband matrix is given by

$$A_M = [cA_{M,n}^1, cA_{M,n}^2, \dots, cA_{M,n}^k] \quad (7)$$

and the detail subband matrix is given by

$$D_m = [cD_{m,n}^1, cD_{m,n}^2, \dots, cD_{m,n}^k] \quad (8)$$

where  $k=12$  is the number of ECG leads and  $m = 1, 2, \dots, M$ . The multiscale matrices contain diagnostic components of the multilead ECG signal. The energy content in the subbands due to wavelet coefficients along each lead is termed as multiscale energy.

$$E_m^d = \frac{1}{N_m} \sum_n |D_{M,n}|^2 \quad (9)$$

$$E_m^a = \frac{1}{N_m} \sum_n |A_{M,n}|^2 \quad (10)$$

It is observed that for all the leads of ECG higher order wavelet subbands ( $cA6, cD6, cD5, cD4$ ) contain large amount of energies and the lower subbands ( $cD3, cD2, cD1$ ) contain less amount of energies. For multiscale matrix the relative energy content of the individual matrix is termed as multiscale

multivariate energy contribution efficiency (MMECE).

$$MMECE_{A_L} = \frac{tr[C_{A_L}]}{tr[C_{A_L}] + \sum_{j=1}^L tr[C_{D_j}]} \quad (11)$$

$$= \frac{E_{A_L}}{E_{A_L} + \sum_{j=1}^L E_{D_j}}$$

$$MMECE_{D_j} = \frac{tr[C_{D_j}]}{tr[C_{A_L}] + \sum_{j=1}^L tr[C_{D_j}]} \quad (12)$$

$$= \frac{E_{D_j}}{E_{A_L} + \sum_{j=1}^L E_{D_j}}$$

### III. RESULT

Here the MI data are taken from the PTB diagnostic ECG database [20]. The 12 lead ECG data are first fed to the preprocessing block. The preprocessing block constitutes filtering method which adopts a moving average filter to remove the base line wanders, muscle artifacts, baseline drifts and powerline interfaces from the multilead ECG recordings. Then the frame based segmentation is carried out to acquire the correlation information between the leads, between the rhythms and between the samples. After the preprocessing the multilead ECG signal is subjected to wavelet transform. Here the six level wavelet decomposition using Daubechies 6/8 biorthogonal filters is adopted.

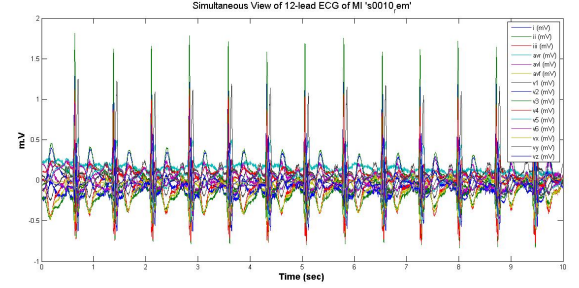


Fig. 3: 12 lead MI ECG data

Fig. 3. represents the 12 lead ECG *s0010\_rem* recording taken from the PTB diagnostic ECG database. The reason for adopting Daubechies 6/8 biorthogonal filters for wavelet decomposition is that, the decomposition scaling function and the wavelet function closely matches the shape of the ECG signal [21], which is shown in Fig. 4.

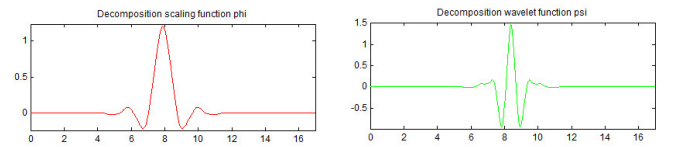


Fig. 4: Scaling and wavelet function of biorthogonal 6/8 filter

Fig. 5. represents the lead I ECG recording of the same MI data. All the 12 lead ECG signal is subjected through wavelet

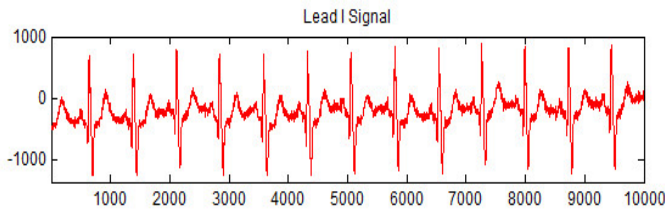


Fig. 5: Lead I of tested MI ECG data

decomposition and the result is shown in Fig.6. The multiscale multivariate energy contribution efficiency (MMECE) of the subband matrices is calculated for different subbands. The MMECE plot of the MI ECG record is shown in Fig.7. The relative energy distribution i.e. energy percentage of all the individual leads are calculated. The subbands cD5, cD6 and cA6 contain more energy whereas the subbands cD1, cD2 and cD3 contain less energy and it is observed that higher order subbands contain more relative energy than lower subbands, which is mentioned in table I for one particular MI case. The higher order subbands contain vital clinical diagnostic information of more energy. Lower order subbands contain relatively less energy due to availability of less clinical information.

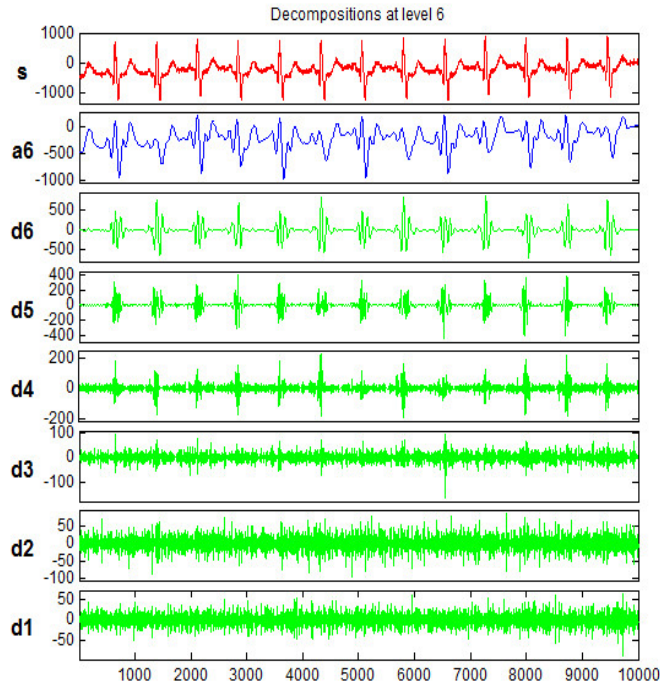


Fig. 6: Six level decomposition of MI case

The within-class variations of normalized multiscale wavelet energy for all ECG leads are evaluated using 1074 MI multilead ECG frames. The results of MI are shown here. The normalized multiscale energy of subband A6 is shown in Fig. 8. Alongwith the normalized multiscale energy of subbands D6, D5 and D4 are presented here as these subbands carry the most vital information. The normalized multiscale energy

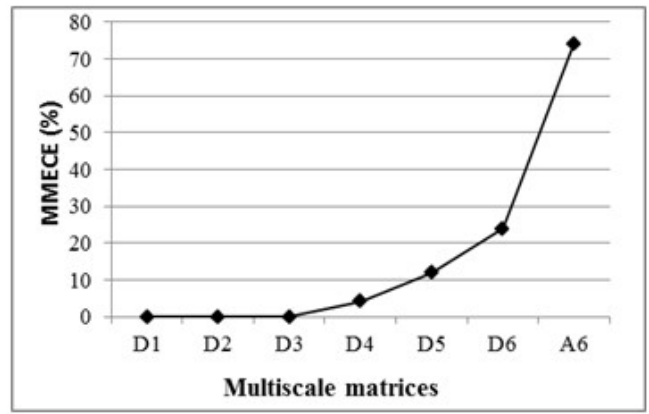


Fig. 7: Energy contribution of multiscale multivariate matrices in terms of MMECE for 12 lead ECG.

TABLE I: Energy percentage distribution of subbands

Lead	EP A6	EP D6	EP D5	EP D4	EP D3	EP D2
I	95.48%	3.38%	0.67%	0.19%	0.20%	0.08%
II	98.08%	1.56%	0.23%	0.06%	0.05%	0.02%
III	97.08%	1.95%	0.76%	0.10%	0.08%	0.03%
aVR	97.22%	2.26%	0.26%	0.10%	0.11%	0.05%
aVL	95.39%	3.14%	1.03%	0.19%	0.17%	0.08%
aVF	98.02%	1.44%	0.43%	0.06%	0.04%	0.02%
V1	91.15%	8.27%	0.50%	0.05%	0.02%	0.01%
V2	73.59%	24.26%	2.01%	0.09%	0.03%	0.01%
V3	72.04%	24.96%	2.84%	0.13%	0.02%	0.01%
V4	70.50%	26.48%	2.79%	0.18%	0.04%	0.01%
V5	86.92%	11.98%	0.88%	0.13%	0.06%	0.02%
V6	92.73%	6.48%	0.55%	0.11%	0.09%	0.03%

of subbands D6, D5 and D4 are shown in Fig. 8, Fig. 9 and Fig. 10.

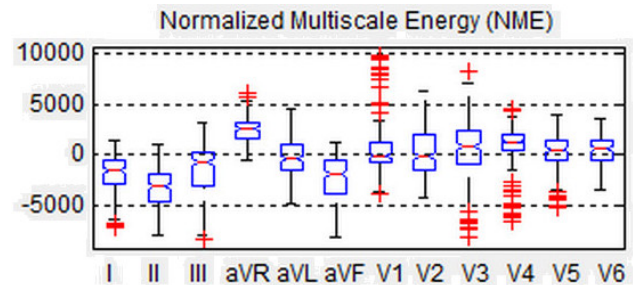


Fig. 8: Variation of multiscale energy for cA6 subbands for 12 ECG leads in MI record

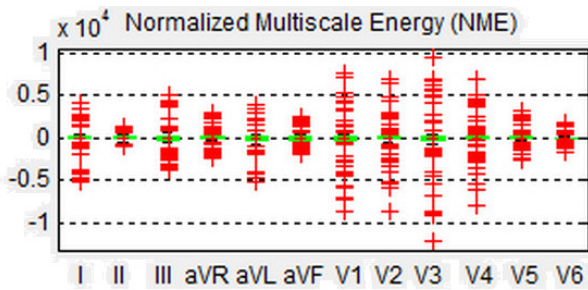


Fig. 9: Variation of multiscale energy for cD6 subbands for 12 ECG leads in MI record

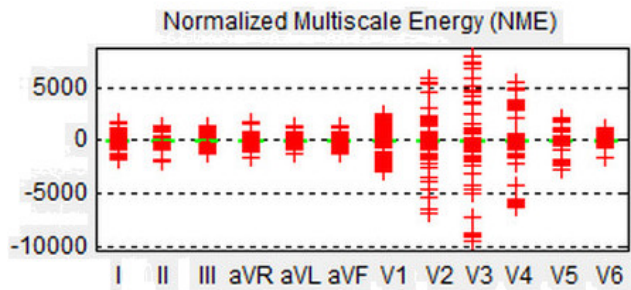


Fig. 10: Variation of multiscale energy for cD5 subbands for 12 ECG leads in MI record

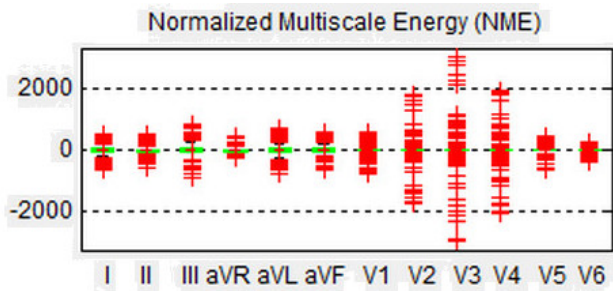


Fig. 11: Variation of multiscale energy for cD4 subbands for 12 ECG leads in MI record

From multiscale wavelet energy analysis it is observed that the mean, standard deviation, median, median absolute deviation and mean absolute deviation are different for different classes. The mean, standard deviation, median, median absolute deviation and mean absolute deviation for the MI class is analysed and given in table.2.

From the table it is observed that there is very large difference between the mean and standard deviation among all the 12 leads of the ECG signal, as all the leads view the heart at different angle. The mean values of leads I, II, III, aVL, aVF, V5 and V6 are very low and it specifies that these leads undergo the infarction in arteries. Inferior MI is depicted from the leads II, III and aVF whereas left lateral MI is traced out from leads I, V5, V6 and aVL. Thus the analysis says that the infarction is an infero-lateral infarction. The standard

TABLE II: . Feature analysis of different leads

Lead	Mean	Standard Deviation	Median	Median Absolute Deviation	Mean Absolute Deviation
I	-212.201	275.515	-205	126	185.104
II	-418.62	255.629	-385	163	203.401
III	-206.42	380.045	-104	196	296.442
aVR	315.379	185.701	305	86	131.023
aVL	-2.39	306.324	142	142	223.317
aVF	-313.017	293.113	-242	172	233.592
V1	79.271	461.078	134	134	269.911
V2	73.563	462.014	212	212	316.341
V3	114.514	610.669	97	209	367.203
V4	111.224	400.628	155	102	216.483
V5	20.904	249.919	55	120	173.689
V6	36.729	187.177	60	116.5	146.800

deviations of corresponding leads are high which confirms the abrupt changes of normal ECG shape.

#### IV. CONCLUSION

In this paper a multiscale energy analysis approach has been adopted for detection of myocardial infarction. Most of the ongoing and present works concentrate on only fewer leads of the ECG signal. Thus it is quite difficult to exactly detect the presence of MI from the ECG recordings. The proposed MI detection technique does not require any prior knowledge of the pathological characteristics of the MI. Here multiscale multilead energy features are taken into consideration for detection of MI. Since all the leads are analysed at one time the simultaneous changes that occur in the leads are properly traced out here. Thus the analysis provides the detection of MI with accurate investigation of all the ECG leads.

#### REFERENCES

- [1] J. E. Hall, *Text Book of Medical Physiology*, 11th ed. New York, NY, USA: Elsevier Health Sciences, 2006.
- [2] A. L. Goldberger, *Clinical Electrocardiography: A Simplified Approach*. New York, NY, USA: Elsevier Health Sciences, 2012.
- [3] D. A. Morrow, *Myocardial Infarction: A Companion to Braunwald's Heart Disease*. New York, NY, USA: Elsevier Health Sciences, 2016.
- [4] S. G. Goodman *et al.*, "The diagnostic and prognostic impact of the redefinition of acute myocardial infarction: lessons from the global registry of acute coronary events (grace)," *American heart journal*, vol. 151, no. 3, pp. 654-660, 2006.
- [5] K. Thygesen *et al.*, "Third universal definition of myocardial infarction," *European heart journal*, vol. 33, no. 20, pp. 2551-2567, 2012.
- [6] J. Martindale and D. F. Brown, *Rapid interpretation of ECGs in emergency medicine: a visual guide*. Lippincott Williams & Wilkins, 2012.
- [7] P. De Chazal, M. O'Dwyer, and R. B. Reilly, "Automatic classification of heartbeats using ecg morphology and heartbeat interval features," *IEEE Transactions on Biomedical Engineering*, vol. 51, no. 7, pp. 1196-1206, 2004.

- [8] S. Mitra, M. Mitra, and B. B. Chaudhuri, "A rough-set-based inference engine for ecg classification," *IEEE Transactions on instrumentation and measurement*, vol. 55, no. 6, pp. 2198–2206, 2006.
- [9] M. Arif, I. A. Malagore, and F. A. Afsar, "Detection and localization of myocardial infarction using k-nearest neighbor classifier," *Journal of medical systems*, vol. 36, no. 1, pp. 279–289, 2012.
- [10] L. Sun, Y. Lu, K. Yang, and S. Li, "Ecg analysis using multiple instance learning for myocardial infarction detection," *IEEE transactions on biomedical engineering*, vol. 59, no. 12, pp. 3348–3356, 2012.
- [11] F. Badilini, M. Merri, J. Benhorin, and A. Moss, "Beat-to-beat quantification and analysis of st displacement from holter ecgs: a new approach to ischemia detection," in *Computers in Cardiology 1992, Proceedings of IEEE*, 1992, pp. 179–182.
- [12] E. Jayachandran *et al.*, "Analysis of myocardial infarction using discrete wavelet transform," *Journal of medical systems*, vol. 34, no. 6, pp. 985–992, 2010.
- [13] C. Papaloukas, D. I. Fotiadis, A. Likas, and L. K. Michalis, "Automated methods for ischemia detection in long duration ecgs," *Cardiovascular Reviews and Reports*, vol. 24, no. 6, pp. 313–319, 2003.
- [14] M. Reddy, L. Edenbrandt, J. Svensson, W. Haisty, and O. Pahlm, "Neural network versus electrocardiographer and conventional computer criteria in diagnosing anterior infarct from the ecg," in *Computers in Cardiology 1992, Proceedings of IEEE*, 1992, pp. 667–670.
- [15] H. Lu, K. Ong, and P. Chia, "An automated ecg classification system based on a neuro-fuzzy system," in *Computers in Cardiology 2000*. IEEE, 2000, pp. 387–390.
- [16] B. Hedén, H. Öhlin, R. Rittner, and L. Edenbrandt, "Acute myocardial infarction detected in the 12-lead ecg by artificial neural networks," *Circulation*, vol. 96, no. 6, pp. 1798–1802, 1997.
- [17] B. R. Bakshi, "Multiscale pca with application to multivariate statistical process monitoring," *AIChE journal*, vol. 44, no. 7, pp. 1596–1610, 1998.
- [18] L. Sharma, S. Dandapat, and A. Mahanta, "Multichannel ecg data compression based on multiscale principal component analysis," *IEEE Transactions on Information Technology in Biomedicine*, vol. 16, no. 4, pp. 730–736, 2012.
- [19] L. Sharma, R. Tripathy, and S. Dandapat, "Multiscale energy and eigenspace approach to detection and localization of myocardial infarction," *IEEE Transactions on Biomedical Engineering*, vol. 62, no. 7, pp. 1827–1837, 2015.
- [20] M. Oeff, H. Koch, R. Bousseljot, and D. Kreiseler, "The ptb diagnostic ecg database," *National Metrology Institute of Germany*, <http://www.physionet.org/physiobank/database/ptbdb>, 2012.
- [21] B. N. Singh and A. K. Tiwari, "Optimal selection of wavelet basis function applied to ecg signal denoising," *Digital signal processing*, vol. 16, no. 3, pp. 275–287, 2006.